1 January 1997

OPTICS COMMUNICATIONS

ELSEVIER

Optics Communications 133 (1997) 393–400

Full length article

Flexible optical implementation of fractional Fourier transform processors. Applications to correlation and filtering

Javier García, Rainer G. Dorsch [1], Adolf W. Lohmann [1], Carlos Ferreira, Zeev Zalevsky [2]

Department Interuniversitari d'Òptica, Facultat de Física, Universitat de València, C/ Doctor Moliner 50, 46100 Burjassot (Valencia), Spain

Received 19 January 1996; revised version received 18 June 1996; accepted 4 July 1996

Abstract

Recently, in the field of fractional Fourier transforms (FRT) an operation coined "fractional correlation" has been proposed and investigated experimentally. In this paper we propose a new setup for obtaining the fractional correlation, which presents several advantages from the experimental point of view. The fractional filter plane can be adjusted accurately with the help of converging beam illumination and using an adjusting device consisting of a combination of Fresnel zone plates. Moreover the scaling factor between the input pattern and the filter can be adjusted at will. This degree of freedom is of special interest when using SLMs. In addition we present a configuration, based on this setup, for spatial filtering of chirp noise in the fractional Fourier domain.

Keywords: Fractional Fourier transform; Fourier transform; Fractional correlation; Correlation; Pattern recognition; Chirp filtering

1. Introduction

The fractional Fourier transform (FRT) has been defined mathematically by Condon [1] in 1937 and extended by Bargman in 1961 [2]. For optical information processing the FRT was re-discovered and implemented by Ozaktas and Mendlovic [3,4] in 1993. Since then a large amount of papers dealing with fractional Fourier appeared. From the optical point of view there exist two different approaches to obtain definitions of an FRT. One definition is based on Hermite-Gaussian-modes (HG) and can be implemented optically by means of GRIN media [4,5]. The other approach is based on rotating the Wigner distribution function of the input signal by a certain angle and can be implemented by means of bulk optical setups [6]. Both definitions can be shown to be equivalent [7]. The definition of the FRT of order P for a given input signal $u(x)$ in the case of bulk optics reads [6]:

$$u_P(x') = \int u(x) \exp\left(\pi i \frac{x^2 + x'^2}{\lambda f_1 \tan\phi}\right) \times \exp\left(-2\pi i \frac{x x'}{\lambda f_1 \sin\phi}\right) \mathrm{d}x, \tag{1}$$

containing an angle ϕ which is related to the fractional order P:

$$\phi = P \times \pi/2. \tag{2}$$

The factor $\sqrt{\lambda f_1}$ acts as a scaling factor between the adimensional variable in the exponential functions

[1] On leave from: Physikalisches Institut, Universität Erlangen, Erwin-Rommel Strasse 1, D-91058 Erlangen, Germany.

[2] Faculty of Engineering, Tel-Aviv University, 69978 Tel-Aviv, Israel.

PII S0030-4018(96)00482-8

and the linear dimensions in both the object and the FRT plane coordinates. It is worth noting that in the Fourier transform case ($\phi = \pi/2$) for each scaling of the input the output will be a differently scaled version of the Fourier transform, i.e. the scaling can be different in input and output planes. On the contrary, in the FRT case, scaling the input results in a FRT of different order (aside from the scaling). To avoid this effect the scaling factors for the input and the output plane must be the same.

Remember that an FRT of order $P = 1$ gives a Fourier transform, an FRT of order $P = 2$ gives inverted imaging and $P = 4$ gives exact imaging. After this definition of the FRT for bulk optics the way was opened to convert systems containing usual or "classical" Fourier transforms into "fractional" Fourier systems. In this spirit the term "fractional correlation" was coined and various theoretical definitions were suggested [8]. The optical implementation of Eq. (1) can be done by using the "type I" and "type II" modules proposed in Ref. [6], which are shown in Figs. 1a and 1b, respectively. A configuration containing a type I module was designed for obtaining the fractional correlation and investigated experimentally in Ref. [9]. In the following the basic expressions for a fractional correlation are given. The classical correlation for two input functions $u(x)$ and $v(x)$ is given by [10]

$$C_1(x_1) = \int u(x) v^*(x - x_1)\, dx = \int \tilde{u}(\nu) \tilde{v}^*(\nu) \exp(2\pi i \nu x_1)\, d\nu, \quad (3)$$

where $\tilde{u}$ and $\tilde{v}$ denote the fractional Fourier transforms of order $P = 1$, which are equal to the classical Fourier transform. Shifting to the fractional correlation we replace the two classical Fourier operations by fractional Fourier transforms:

$$\tilde{u}(\nu) \to u_P(x'), \quad \tilde{v}(\nu) \to v_P(x'), \quad (4)$$

where the x' includes the previously discussed scaling factor. The final inverse Fourier transform of Eq. (3) to obtain the correlation peak remains unchanged. The use of different orders for every transform involved in the process (FRT for input, reference and the final transformation of the product), yields different, but still valid definitions of the fractional correlation [8]. In the following we will deal with the above

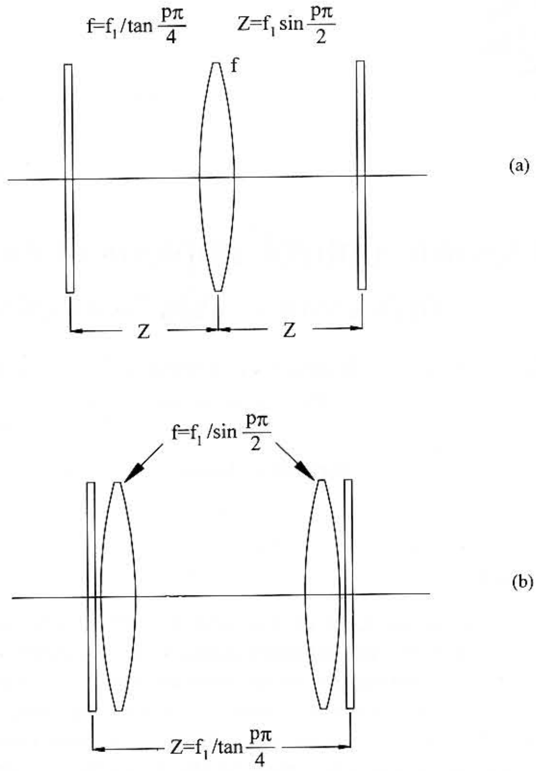

Fig. 1. Optical setups for obtaining an FRT, (a) type I module, (b) type II module.

described definition. An extension for a general case is straightforward. The optical setup for this fractional correlation contains two type I modules of Fig. 1a in cascade. The first one with fractional order $P \neq 1$ and the second with order $P = -1$.

Because the FRT contains information of the frequency domain as well as of the object domain, the fractional correlation is expected to provide different features as compared to the classical correlation. One property is the shift variance of the fractional correlation [9]. A peak is obtained only if the input object is in (or near) the exact position x_{exact}. The range of this position where a correlation peak still appears in the output plane of the fractional correlator is a function of the fractional order [11]. This range can be estimated by means of the phase mismatch in the FRT plane. Assuming that the phase difference between the fractional Fourier transforms of the input at its original position and the displaced input is smaller than a fixed value (π was taken for convenience), it can be shown that the difference between the exact position and the actual position must satisfy the following inequality:

$$|x_{\text{exact}} - x| < \lambda f_1 |\tan\phi| / \Delta x, \tag{5}$$

where Δx denotes the object's size. This estimation is an upper bound, the actual range may strongly depend on the geometry of the object.

For orders close to $P = 1$ this range is large and therefore almost shift invariant like the classical correlator. For low orders close to $P = 0$ this range is very narrow and the shift variant property of the fractional correlator is more crucial. Therefore if it is desired to detect the location of the object with an accurate precision a low fractional order has to be implemented.

The disadvantage of the setup discussed above from the experimental point of view occurs in finding the exact fractional Fourier plane at distance z where the filter should be placed at, for a given focal length of the lens (f) [6]:

$$\begin{aligned} z &= f_1 \sin(P\pi/2) \\ &= \tan(P\pi/2) f \sin(P\pi/2). \end{aligned} \tag{6}$$

There are several experimental drawbacks in the original setup. The first one is that, when dealing with thick lenses, the principal planes are not accurately known. On the other hand measuring distances accurately on an optical bench is a problem, in general. An additional problem is that the experimentalist has no hint in hand to recognize whether he is in the right FRT-plane or not. The fractional Fourier pattern does not show any special features as the classical Fourier pattern. The main disadvantage is that the scales of the input object and the filter are fixed. In addition the fractional order is determined by the system, requiring a complex rearrangement if a different order is needed. A "fake zoom" system was proposed for achieving a variable FRT order, at the price of increasing the number of lenses in the system [12]

With all this in mind we want to propose a modified setup for obtaining a fractional correlation that bypasses all the above mentioned problems. Such a setup would have as a main advantage an accurately adjustable filter plane, in axial position, as well as in scale. The main idea of this setup is to use a convergent beam illumination and an adjusting device. This device is essentially a combination of Fresnel zone plates (two-dimensional chirp functions). In the following we will explain the underlying idea in terms of Wigner optics. A more detailed description of the effect of FRT on chirp functions is given in Ref. [13].

In the 2D Wigner domain of a 1D function, a tilted line delta function crossing the origin of the (x, v) plane will result in a symmetrical chirp. This is, a spatial distribution with a frequency that increases linearly from the origin. For a 2D distribution, this is known as a Fresnel zone plate pattern. For a two-dimensional input function the corresponding Wigner domain becomes four-dimensional. Therefore, for the sake of simplicity, we restrict ourselves to the 1D case. Taking into account that the FRT is a separable transformation, a generalization to two dimensions is straightforward. A fractional Fourier transform can be associated with a rotation of the Wigner distribution function (WDF) by an angle connected to the FRT order. Thus, in the spatial domain, the FRT tool can transform a chirp (or equivalently a Fresnel zone plate) into a delta function and vice versa.

In the following the underlying theory is explained briefly. The Wigner transform of a one-dimensional function $u(x)$ is defined by

$$\begin{aligned} W(x,\nu) &= \int u(x + x'/2) u^*(x - x'/2) \\ &\quad \times \exp(-2\pi i \nu x')\, dx', \end{aligned} \tag{7}$$

where x represents the space coordinate and ν represents the spatial frequency. The inversion from the WDF to the signal is unique, apart from a constant factor:

$$\int W(x,\nu) \exp(4\pi i x \nu)\, d\nu = u(2x) u^*(0). \tag{8}$$

Some examples of WDFs are:

Pulse:

$$u(x) = \delta(x - x_0) \Rightarrow W(x,\nu) = \delta(x - x_0). \tag{9}$$

Monofrequency:

$$u(x) = \exp(2\pi i \nu_0 x) \Rightarrow W(x,\nu) = \delta(\nu - \nu_0). \tag{10}$$

A linear increasing frequency or chirp function is given in coordinate space and after transformation to the Wigner domain by

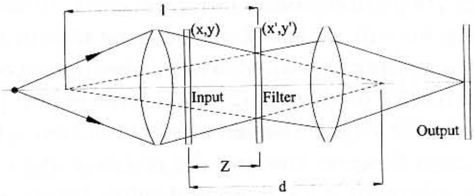

Fig. 2. Adjustable fractional Fourier correlator.

$$u(x) = \exp[2\pi i(b_2x^2/2 + b_1x + b_0)]$$
$$\Rightarrow W(x,\nu) = \delta(b_2x + b_1 - \nu). \quad (11)$$

Therefore a 1D-delta function corresponds to a vertical line in the Wigner domain. A single frequency corresponds to a horizontal line, while a chirp function corresponds to a slanted line. Thus, a $\pi/2$ rotation operation in the Wigner domain transforms a pulse to a monofrequency function, passing trough chirp functions.

The fractional Fourier transform of order P is associated with a rotation of the WDF by an angle of $\phi = P \times \pi/2$ as given in Eq. (2). Expressed implicitly by

$$\mathcal{W}[\mathcal{F}^P(u)] = R_{-\phi}\mathcal{W}[u], \quad (12)$$

where R_ϕ denotes a counterclockwise rotation of a two-dimensional function and $\mathcal{W}[u]$ is the Wigner transform of $u(x)$. Eqs. (11) and (12) imply that by performing an FRT of a certain order P, a chirp term can be transformed into a delta function and vice versa. This permits the spatial filtering of chirp noise in a fractional domain. The fractional order P to obtain this relationship is determined by

$$\phi = \tan^{-1} b_2. \quad (13)$$

In Section 2 we introduce the modified setup for performing the fractional correlation. Experimental results are shown and compared with computer simulations. Section 3 discusses a similar setup for spatial filtering of chirp noise in a fractional Fourier domain.

2. Modified setup for fractional correlation

The basic idea of the modified setup lies on a variable scale inexact fractional Fourier transformer. A scheme of it is shown in Fig. 2. Comparing with the module of Fig. 1b (type II FRT module) the differences are that the second lens in front of the fractional Fourier plane is removed and the effect of the first lens is accomplished by illuminating the input transparency with a spherical beam. The axial distance where the beam converges, d, is equivalent to the focal distance f in the type II setup. This produces an FRT that is in fact multiplied by a diverging quadratic phase factor. These quadratic phase factors (paraxial approximations of spherical waves) can be eliminated if the input and the output are considered to be on two spherical reference surfaces. An interpretation of the FRT based on this idea can be found in the literature [14,15].

If in the FRT plane a filter matched to an exact FRT is positioned then the phase of the optically obtained FRT will be cancelled, remaining just a quadratic phase factor that can be focused by an additional lens without any special characteristics. In order to prove this we can calculate the pattern in the filter plane (x', y') diffracted by the object transparency $u(x, y)$ and compare it with the FRT expression (Eq. (1)). The amplitude just after the transparency, for the one-dimensional case, is given by

$$u_1(x) = u(x)\exp\left(-i\frac{\pi x^2}{\lambda d}\right). \quad (14)$$

After Fresnel diffraction by a distance Z, the amplitude results:

$$u_2(x') = \exp\left(i\frac{\pi}{\lambda Z}x'^2\right) \times \int_{-\infty}^{+\infty} u(x)\exp\left[i\frac{\pi}{\lambda}\left(\frac{1}{Z} - \frac{1}{d}\right)x^2\right] \times \exp\left(-i\frac{2\pi}{\lambda Z}xx'\right)\,dx. \quad (15)$$

As stated in the introduction the aim of this paper is to design a setup for obtaining a variable scale FRT. In order to check this let us consider the amplitude distribution of the FRT of order P of $u(x)$, when the output plane is scaled by a factor a:

$$u_P(x'/a) = \exp\left(i\pi\frac{x'^2}{\lambda f_1 a^2 \tan\phi}\right) \times \int u(x)\exp\left(i\pi\frac{x^2}{\lambda f_1 \tan\phi}\right) \times \exp\left(-2\pi i\frac{xx'}{\lambda f_1 a \sin\phi}\right)\,dx. \quad (16)$$

Note that the $\sqrt{\lambda f_1}$ scaling factor affects equally both input and output linear variables (x and x' respectively), while the a factor only scales the output distribution, without altering the input one. Comparing Eqs. (15) and (16) we see that the integrals in both expressions match, provided the following conditions are fulfilled:

$$\frac{1}{Z}-\frac{1}{d}=\frac{1}{f_1\tan\phi},\quad \text{and } Z=f_1 a\sin\phi. \tag{17}$$

With this changes, Eq. (15) can be rewritten as

$$u_2(x')=\exp\left[i\frac{\pi}{\lambda Z}\left(1-\frac{1}{a}\right)x'^2\right]\times\exp\left(i\frac{\pi}{\lambda d a^2}x'^2\right)u_p(x'/a). \tag{18}$$

We see that the optically obtained distribution equals the scaled FRT function, except for a global quadratic phase factor. This factor is the paraxial approximation of a spherical beam diverging from a distance:

$$l=a^2\frac{Zd}{Z+d\left(a^2-1\right)}. \tag{19}$$

In the particular case of $a=1$ the phase factor diverges from a distance d, as expected from the qualitative description of the setup.

The main advantage of this setup with respect to previous ones is that the scale between the input pattern and the filter recorded on the plate can be adjusted at will. This possibility is of special importance when SLMs are used for either the input or the filter transparency. In this case the size of the transparencies cannot be changed arbitrarily, the scale matching relying on the setup. The main action to be performed is a longitudinal movement of the object transparency along the z axis. This changes the convergence of the quadratic phase factor illuminating the transparency. According to the first condition in Eq. (17) this will change both the global scaling factor, f_1, and the fractional order, given by ϕ. An adjustment of the distance, Z, between the input and the filter plane will fix the FRT plane for the desired scaling factors and order. After the action of the filter it is necessary to perform a Fourier transform of the FRT plane. Under the above defined assumptions the proposed setup produces the product of the FRT and the filter function, illuminated by a spherical beam diverging from an axial point located at distance l from the filter plane. If a lens is introduced forming an image of this point, in the plane of the image the correlation will be obtained. The output will be also affected by a quadratic phase factor, that can be neglected if an intensity detector is used.

The flexibility of adjusting the system has been increased by defining a procedure for matching the sizes of the optically obtained FRT and the filter. For this purpose a transparency containing a set of chirp functions (that for the 2D case are zone plates) and with a size equal to that of the input scene is prepared. The chirps are obtained by inverse FRT of a set of isolated dots, with the desired fractional order. Also a transparency with the FRT of the chirps (consisting on isolated dots) is prepared with the same scale factor as the CGH used to record the filter. Checking the matching of the dots with the optically obtained FRT of the chirps the perfect scaling adjustment is obtained. The setup of Fig. 2 is not the only possible one. It provides a FRT with an additional quadratic phase factor. This permits the adjustment of distances to match the size. A similar setup may be prepared that produces an FRT without any additional phase factor. Nevertheless, in this case the magnification of the FRT would be fixed. It is also worthwhile to note that if a joint transform fractional correlator is used, i.e. if the input transparency contains both the target and the scene, then the quadratic phase factor affects the full joint spectrum. When the joint spectrum is recorded in intensity it has no influence in the output plane. Then this FRT joint correlator would be equivalent to a misfocused conventional JTC [16].

3. Adjustment procedure and experimental results

3.1. Fractional correlation

In order to detail the adjustment procedure, in this section the steps for performing a fractional correlation are described. The setup used in the experiment is shown in Fig. 2. The goal is to obtain a fractional correlation with order $P=0.5$. The input image used in the optical and computer experiments is shown in Fig. 3a. It is a 256×256 binary image taken from a CCD camera. The filter is prepared for the detection of the upper screw (marked with an arrow in the fig-

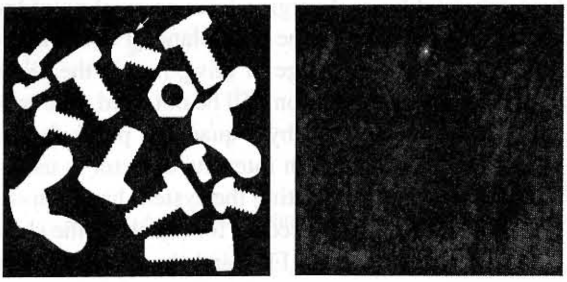

(a) (b)

Fig. 3. (a) Input scene for the fractional correlator. The target is indicated with an arrow. (b) Digital fractional correlation obtained for $P = 0.5$.

ure) as a Detour Phase type computer generated hologram [18]. An FRT of order $P = 0.5$ is computed and its amplitude and phase are coded in the hologram. The algorithm used to calculate the FRT is based on Hermite–Gaussian functions and was introduced in Ref. [17]. Both, the input image and the hologram are printed in a laser printer and photoreduced down to approximately 10 mm size. The pixel size in the input transparency defines the global scaling parameter, f_1, equal for input and filter. In our setup, we will match the f_1 value of the system to the one of the transparencies. The ratio between the global size of the input and the hologram determines the relative scaling parameter, a, of the output. This is a fixed parameter, independent of f_1. For the sake of later comparison a computer simulation of the fractional correlation is depicted in Fig. 3b. A distinct correlation peak corresponding to the target in the upper part of the image can be seen. The other two objects, identical to the target, are not detected owing to the distance from the target and the shift variance of the procedure.

The first step in the setup contains a point source connected with a lens to produce a convergent beam. Therefore the degree of convergence is adjustable easily by changing the parameter d, which means moving the input transparency along the axis. Once the order (P), the relative scaling factor, a, and the distance d have been established, the distance between input and FRT planes, Z, is given by Eq. (17). This distance can be expressed as

$$Z = d(1 + a\cos\phi). \qquad (20)$$

Every pair of distances (Z, d), is connected with a different scaling parameter f_1. Now it is necessary to select the proper pair of distances that will match the sizes of input and filter transparencies. To get started we generate an image with three delta-peaks and digitally performed an inverse FRT of order $P = -0.5$. This results in a three overlapping Fresnel zone plates pattern. On the other hand we prepare the three delta-functions as a transparency. Hence placing the Fresnel zone plates pattern into the converging beam we can find the proper FRT plane of order $P = +0.5$ at distance Z by adjusting the distance d and matching the transparency with the optically obtained delta-peaks. Note that at least two delta-peaks have to be on the mask in order to obtain exact matching of both scales. This matching can be obtained quite accurately by magnifying this plane onto a CCD-chip while adjusting. The proper FRT plane is now fixed and the filter for the fractional correlation is placed there. The filter is computed with the above mentioned HG functions algorithm, and it is displayed with the same pixel size than the adjusting transparency containing the delta functions. Hence, the filter matches with the optically fractional transformed input pattern except for a quadratic phase which produces a divergent beam after the fractional correlation. This beam diverges from a distance l, according to Eq. (19). Therefore the last step of the setup is to focus the divergent beam to obtain the final correlation peak. Neither for the FRT stage, nor for the second Fourier transformer it is demanded any special characteristics for the lens. Using a lens the correlation is focused on a CCD camera and the intensity is recorded in a computer by means of a frame grabber. The experimental output is shown in Fig. 4. It agrees well with our computer simulations (Fig. 3(b)). For the sharpness of the fractional correlation peak (PCE) we con-

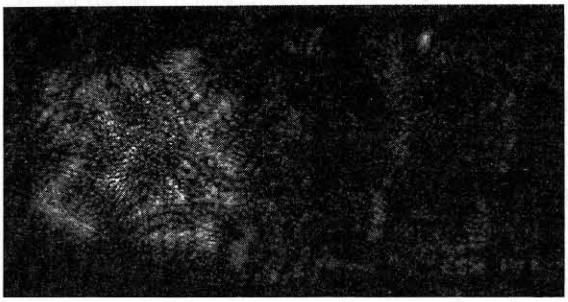

Fig. 4. Experimental output of the adjustable fractional Fourier correlator.

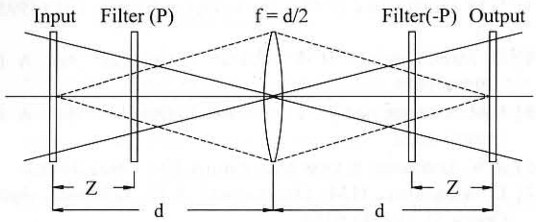

Fig. 5. Modified setup for performing chirp filtering.

sider the following. Generally speaking the larger the extensions of the transformed object in the fractional domain the smaller the extension of the output will be after the final Fourier transform. This is related to the scaling property of the Fourier transform. An additional advantage of our modified setup is that it can be adjusted for any fractional correlation order without changing the focal length of the lens. This would be unavoidable for a fractional correlator consisting of type I or type II modules [17].

3.2. *Fractional spatial filtering*

A similar idea can be applied for chirp filtering. If the scene is corrupted by a chirp noise, it would be impossible to remove it in either Fourier or in spatial domain. The chirp, on the contrary, will be well focused in a FRT plane. Thus a spot in the proper fractional domain (at the P value that concentrates the chirp) will completely remove the noise.

For filtering chirp background noise we introduce a similar modified setup to the one discussed above. The illuminating part of this modified filtering setup is equivalent to the one in Fig. 2. Chirp filtering with a setup containing type I modules was described in Ref. [13]. With our modified configuration shown in Fig. 5 we can adjust again the FRT-plane, this time for spatial filtering. Here we prepare an input pattern similar to Fig. 3a but with a three Fresnel zone pattern as background noise (see Fig. 6a). The Fresnel zone plate pattern will focus in the fractional Fourier plane of order $P = +0.8$ leading to three delta peaks. Here we prepare a filter with three band stop dots of equal spacing. Because our input pattern is a real function we have to filter for the order $P = -0.8 \equiv 2 - 0.8 = 1.2$ in addition [13]. This is implemented by setting a lens of focal length $f = d/2$ in the Fourier plane of the convergent beam. This condition is not restrictive,

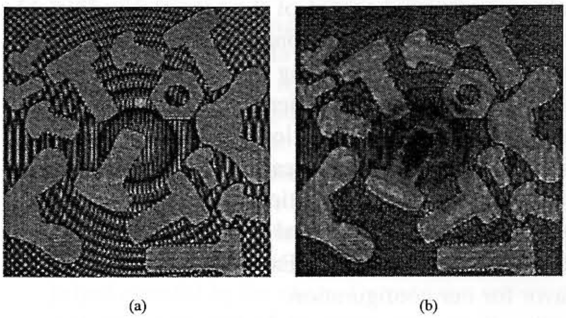

Fig. 6. Example of chirp noise removal. (a) Input scene of Fig. 3a with chirp noise as background. (b) Experimental output after filtering the chirp background noise.

as the parameter d can be varied by the position of the first lens. Imaging of the input transparency is obtained at the rear focal plane at distance d (4f-setup). As stated above imaging is equivalent to an FRT of order $P = 2$. Hence, the plane of an FRT of order $P = 2 - 0.8$ of the input object is located at the same absolute distance z for order $P = +0.8$ but now measured from the output plane according to the divergent beam after the lens. Note that this setup is totally symmetrical for the two filter planes with respect to the Fourier plane and therefore both filters have equal size. The experimental output obtained after removing the chirps in the two fractional planes is shown in Fig. 6b. It agrees well with computer simulations.

The removing of the central chirp distorts the inner part of the image due to cutting information in the central regions of the fractional planes. There the delta peak and the fractional transform of the input object are overlapped, and it is impossible to remove the chirp without blocking a small part of the FRT of the input pattern. On the contrary the outer chirps are totally spatially separated in the fractional domain according to their out of center location. After filtering no information of the object is lost in this case. The outer parts of Fig. 6b are well reconstructed, with the only artifacts due to the coherent illumination and experimental sources of noise.

4. Conclusions

In this paper we introduce a modified optical setup for the implementation of the fractional correlation. This setup beats the previous ones from the experimental point of view because of the accurately adjustable fractional filter plane. It contains convergent beam illumination and an adjusting device for localization of the proper fractional Fourier plane. The main advantage of the modified fractional correlator lies in the freedom of adjusting the scale between the input pattern and the filter. In addition the same setup can be used for different fractional orders without changing the lenses' focal lengths. Experimental results are in favor for our configuration.

Based on the same principle, a setup for spatial fractional filtering of chirp noise is proposed. Experimental results are presented, for both fractional correlation and chirp noise removal.

Acknowledgements

This work was supported by Spanish Comision Interministerial de Ciencia y Tecnologia, under the project TAP93-0667-103-03.

References

[1] E.U. Condon, Proc. Nat. Acad. Sci., USA 23 (1937) 158.
[2] V. Bargmann, Comm. Pure Appl. Math. 14 (1961) 187.
[3] H.M. Ozaktas and D. Mendlovic, Optics Comm. 101 (1993) 163.
[4] D. Mendlovic and H.M. Ozaktas, J. Opt. Soc. Am. A 10 (1993) 1875.
[5] H.M. Ozaktas and D. Mendlovic, J. Opt. Soc. Am. A 10 (1993) 2522.
[6] A.W. Lohmann, J. Opt. Soc. Am. A 10 (1993) 2181.
[7] D. Mendlovic, H.M. Ozaktas and A.W. Lohmann, Appl. Optics 33 (1994) 6188.
[8] D. Mendlovic, H.M. Ozaktas and A.W. Lohmann, Appl. Optics 34 (1995) 303.
[9] D. Mendlovic, Y. Bitran, R.G. Dorsch and A.W. Lohmann, J. Opt. Soc. Am. A 12 (1995) 1665.
[10] A. Vander Lugt, IEEE IT-10 (1964) 139.
[11] A.W. Lohmann, Y. Bitran and D. Mendlovic, About the space-variance of FRT correlators, Appl. Optics (submitted).
[12] A.W. Lohmann, Optics Comm. 115 (1995) 437.
[13] R.G. Dorsch, A.W. Lohmann, Y. Bitran, D. Mendlovic and H.M. Ozaktas, Appl. Optics 33 (1994) 7599.
[14] P. Pellat-Finet and G. Bonnet, Optics Comm. 111 (1994) 141.
[15] H.M. Ozaktas and D. Mendlovic, J. Opt. Soc. Am. A 12 (1995) 743.
[16] F.T.S. Yu, C. Zhang, Y. Jin and D.A. Gregory, Optics Lett. 14 (1989) 922.
[17] Y. Bitran, R.G. Dorsch, A.W. Lohmann, D. Mendlovic and H.M. Ozaktas, Appl. Optics 34 (1995) 1329.
[18] A.W. Lohmann and D.P. Paris, Appl. Optics 6 (1967) 1739.